BENDING OF COMPOSITE PLATE UNDER MAGNETIC FIELD

Piotr Kędzia[1a], Zbigniew Kosma[2]

[1] Faculty of Mechanical Engineering and Management, Poznan University of Technology, Poland
[2] Institute of Applied Mechanics and Power Engineering, University of Technology and Humanities in Radom
[a]piotr.kedzia@put.poznan.pl, [b]zbigniew.kosma@uthrad.pl

Summary

The main objective of presented study is composite rectangular plate subjected to load generated by magnetic field. The field changes around the area limited by magnetic elements. The plate is made of polyethylene and consists of three layers: two faces and porous core. The core is filled with ferrofluid. Porous structure prevents fluid from flowing out between cells in the middle plane. The load influences perpendicular to the plate and along middle plane.The load is generated by the system build of Helmholtz and Golay coils which are frequently used in modern MRI tomographs (Magnetic Resonance Imaging). Bending of the plate is affected by the magnetic field which influences on ferrofluid in porous cells. The function of bending of the plate is approximated by bicubic spline function presented by normalized *B*-spline functions. Required approximations of partial derivatives appearing in equation of bending of the plate and in boundary conditions are obtained with the property, that bicubic spline function is polynomial spline function respect to each of independent variable separately. Efficiency of these algorithms is proved by comparing test results with numerical simulations, with FEM in Autodesk Simulation v.14 program. Prepared numerical algorithm determines bending of the plate under applied load which is induced by spatial changes of magnetic field.

Keywords: ferrofluid, plate, magnetic field, magnetic coils

ZGINANIE PŁYTY KOMPOZYTOWEJ W POLU MAGNETYCZNYM

Streszczenie

Przedmiotem badań jest kompozytowa płyta prostokątna poddana obciążeniu wywoływanemu przez zmienne w przestrzeni pole magnetyczne. Płyta jest wykonana z polietylenu i składa się z trzech warstw: dwóch okładzin zewnętrznych oraz porowatego rdzenia, wypełnionego płynem ferromagnetycznym. Porowata struktura płyty zapobiega przelewaniu się płynu ferromagnetycznego wzdłuż płaszczyzny środkowej. Obciążenie działające jednocześnie prostopadle do powierzchni płyty oraz wzdłuż płaszczyzny środkowej wywołane jest przez cewki Helmholtza oraz cewki Golaya stanowiące podstawowy trzon układu magnesów współczesnych tomografów do obrazowania MRI (Magnetic Resonance Imaging). Wygenerowane pole magnetyczne tomografu poprzez oddziaływanie na płyn ferromagnetyczny wywołuje ugięcie płyty. Funkcję ugięcia płyty aproksymowano bikubiczną funkcją sklejaną przedstawioną przez znormalizowane *B*-funkcje sklejane. Niezbędne aproksymacje pochodnych cząstkowych występujących w równaniu ugięcia płyty i w warunkach brzegowych uzyskano, korzystając z własności, że bikubiczna funkcja sklejana jest wielomianową funkcją sklejaną względem każdej zmiennej niezależnej z osobna. Skuteczność algorytmów została w pełni potwierdzona poprzez porównanie wyników obliczeń testowych z symulacjami numerycznymi wykonanymi metodą elementów skończonych za pomocą programu Autodesk Simulation v.14. Przy wykorzystaniu opracowanej metody numerycznej wyznaczone zostały ugięcia płyty z uwzględnieniem przestrzennych zmian natężenia pola magnetycznego podczas jej zginania.

Słowa kluczowe: ferrofluid, płyta warstwowa, pole magnetyczne, cewki magnetyczne

1. INTRODUCTION

Bending of the plates was described in many papers by various amount of researchers, but most of them focus on one particular problem.

Applications of plates in areas such as aircrafts, space industry indicate, that the problem is still actual nowadays. The difference is that these problems are more complex. The plates are multi-layered structures, generally with porous cores etc. Doyle (2001) presented mathematical models of thin-walled structures and problems of their statics, dynamics and stability. A comprehensive review of the issues of strength, stability and dynamics of the plates and coatings is presented in the monograph edited by Wozniak (2001). Ventsel and Krauthammer (2001) described in details theory, analysis and applications of thin plate and shells. More complex problems occur, when different areas of research are taken under consideration, e.g. when plates are build of composites or smart materials. Such materials are mainly build as magnetic materials. The methods of manufacturing as well as the properties of magnetic structures were described by Kaleta (2013). Rosensweig defined in his monograph ferromagnetic fluids, which are of particular importance in smart materials research in many fields of industries. You-He and Xiaojing (1997) derived general expression of magnetic force for soft ferromagnetic plates in complex magnetic fields. Hasanyan and Harutyunyan (2009) described magnetoelastic interactions in a soft ferromagnetic body with a nonlinear law of magnetization. Ambartsumian, Bagdasarian and Belubekian similarly considered magnetoelasticity of thin shells and plates. Control of magnetic field in so called smart plates was presented by Nguyen and Tong (2007) as well as by Sun and Tong (2005). Kędzia and Magnucki (2014) described stability of the plate contained pockets filled with ferrofluid placed in magnetic field of tomograph coils (Czechowski et al. 2013).

The objective of the study is a rectangular plate made of polyethylene with the length a, the width b and the thickness h. The plate (Fig. 1) is cellular structure (e.g. honeycomb structure), where each cell is filled with ferrofluid. Such construction is assumed to avoid ferrofluid to flow from flowing out between cells in the middle plane, but in further part of the paper homogenization of the plate is taken into account. The plate is placed into the magnetic systems of coils, which is build of two subsystems: the main magnetic field system - Helmholtz coil (Fig. 2) and transverse gradient magnetic field - Golay coils (Fig. 3). The Helmhotz coils consists of two wire loops, with a radius - r each and distance between them - r. They are characterize by homogeneous magnetic field. Relative error for that system is less than 5 ppm (parts per million) with respect to the distance of about half a radius r from the centre of the system of coils. The second subsystem consists of four "saddles" with the radius of arcs r. Homogeneity of transverse gradient magnetic field is not as good as in case of Helmholtz coils and it is less than $5\,\%$ with respect to the distance of $1/3$ of the radius r from the centre of the system of coils.

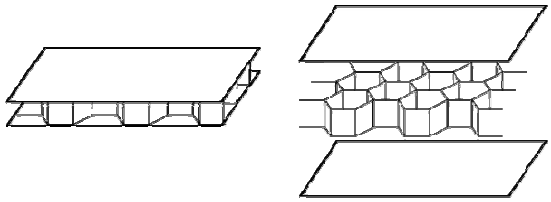

Fig. 1. Cellular structure of the plate

Both systems of coils generate magnetic field which changes around the area limited by magnetic elements

$$\begin{aligned} &\mathbf{H} = \left[H_x + h_{x,z} \cdot z, 0, h_{z,x} \cdot x\right] \\ &H_x{}^0 = const. \\ &h_{z,x} = h_{x,z} = const. \end{aligned} \quad , \tag{1}$$

where H_x is the magnetic field generated by Helmholtz coils and $h_{x,z}$ and $h_{z,x}$ are concomitant transverse gradient magnetic fields generated by Golay coils. Presented systems of coils are used in MRI (Magnetic Resonance Imaging). Helmholtz coils (or modified versions of it) are used to generate main magnetic field and gradient coils, including Golay coils, are used to change spatial distribution of magnetic field in linear function in specific direction. Construction of thomograps, dependent on the method of imaging, is often manufactured of plastic. It allows to avoid the edge currents which affect some perturbation on imaging technique.

The aim of the paper is to designate how the magnetic fields, generated by two subsystems of magnetic coils, influence on bending of the plate filled with ferrofluid. Ferrofluids do not conduct currents, so it is assumed that magnetic field acts only on ferrofluid and induces Kelvin force. This force influences on the plate so mechanical force is considered. That assumption makes that the coupled mechanical and magnetic problem is not taken into consideration.

The magnetic field generated by the coils induces Kelvin force in ferrofluid

$$\mathbf{n} = \frac{1}{2}\mu_0 \chi (1-\chi) \nabla H^2 , \tag{2}$$

where μ_0 is magnetic permeability, χ is magnetic susceptibility.

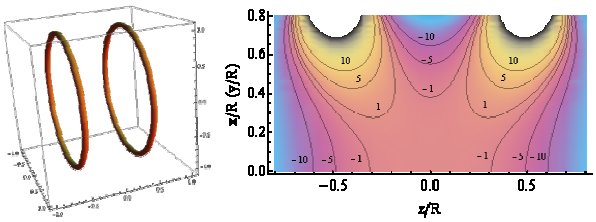

Fig. 2. Helmholtz coils with its homogeneity in ppm

Ferrofluid influences on the cellular plate where the forces along the middle plane in one direction n_x and perpendicular to the plate n_z are defined in the following way

$$\begin{aligned} n_x &= h\cdot\int_0^x \mu_0\chi(1-\chi)h_{z,x}^2\cdot t\,dt \\ &= \frac{1}{8}\mu_0\chi(1-\chi)h_{z,x}^2\cdot x^2 h \\ n_z &= h\mu_0\chi(1-\chi)\left(h_{x,z}^2\cdot z + H_x\cdot h_{x,z}\right) \end{aligned} \quad . \tag{3}$$

Force n_x depends on x component and force n_z depends on z component, so calculated deflection should actualize magnetic field.

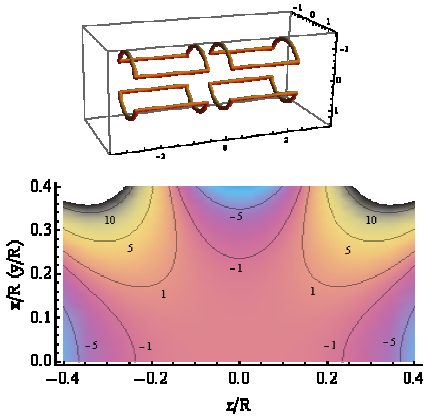

Fig. 3. Golay coils with its homogeneity in %

In above formulae magnetic fields are considered to be homogeneous (both main and gradient).

2. NUMERICAL ALGORITHM

In this study, classical theory of the plate is applied. Deflection $w = w(x,y)$ of the plate (Fig. 4) is defined in the following form:

$$\begin{aligned} &\frac{\partial^4 w}{\partial x^4} + 2\frac{\partial^4 w}{\partial x^2\partial y^2} + \frac{\partial^4 w}{\partial y^4} = \\ &= \frac{1}{D}\left(q + n_x\frac{\partial^2 w}{\partial x^2} + n_y\frac{\partial^2 w}{\partial y^2} + 2n_{xy}\frac{\partial^2 w}{\partial x\,\partial y}\right), \end{aligned} \tag{4}$$

where

$$D = \frac{E h^3}{12\left(1-\nu^2\right)},$$

with E - Young's modulus, ν - Poisson's ratio.

The boundary conditions are

- $$w = 0, \quad \frac{\partial w}{\partial n} = 0, \tag{5}$$

  for clamped edge (n - normal vector),

- $$w = 0, \quad \frac{\partial^2 w}{\partial n^2} = 0, \tag{6}$$

  for simply supported edge.

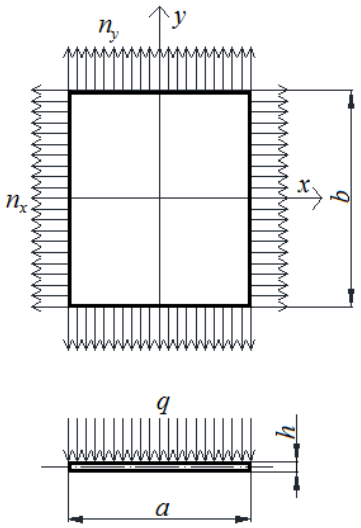

Fig. 4. Load of plate

The square mesh was generated to solve eq. (4) with boundary conditions (5)-(6) for rectangular plate in xy plane. Each point of mesh is defined

$$\begin{aligned} &x_i = i\,h,\ \ i = -1,0,1,\ldots,N+1; \\ &y_j = j\,h,\ \ j = -1,0,1,\ldots,M+1; \quad h = \frac{a}{N} = \frac{b}{M}. \end{aligned} \tag{7}$$

The function of bending of the plate is approximated by the bicubic spline function

$$w(x,y) \approx \sum_{i=-1}^{N+1}\sum_{j=-1}^{M+1} \tilde{q}_{i,j}\, B_i(x)\,\tilde{B}_j(y), \tag{8}$$

presented by known normalized B-spline functions $B_i(x)$ and $\tilde{B}_j(y)$ defined by formulas:

$$B_k(x) = B(x - x_k);$$

$$B(x) = \frac{1}{6h^3}\begin{cases} 0 & \text{for } x \le -2h, \\ (x+2h)^3 & \text{for } -2h \le x \le -h, \\ -3x^3 - 6x^2 h + 4h^3 & \text{for } -h \le x \le 0, \\ 3x^3 - 6x^2 h + 4h^3 & \text{for } 0 \le x \le h, \\ (2h-x)^3 & \text{for } h \le x \le 2h, \\ 0 & \text{for } x \ge 2h \end{cases}$$

and unknown coefficients $\tilde{q}_{i,j}$. Essential approximations of partial derivatives, appearing in equation of bending of the plate and in boundary conditions, are obtained with the property, that the bicubic spline function (7)-(8) is the polynomial spline function with respect to each of independent variables separately. Schemes of the function of deflection and its derivatives are presented in Fig.5.

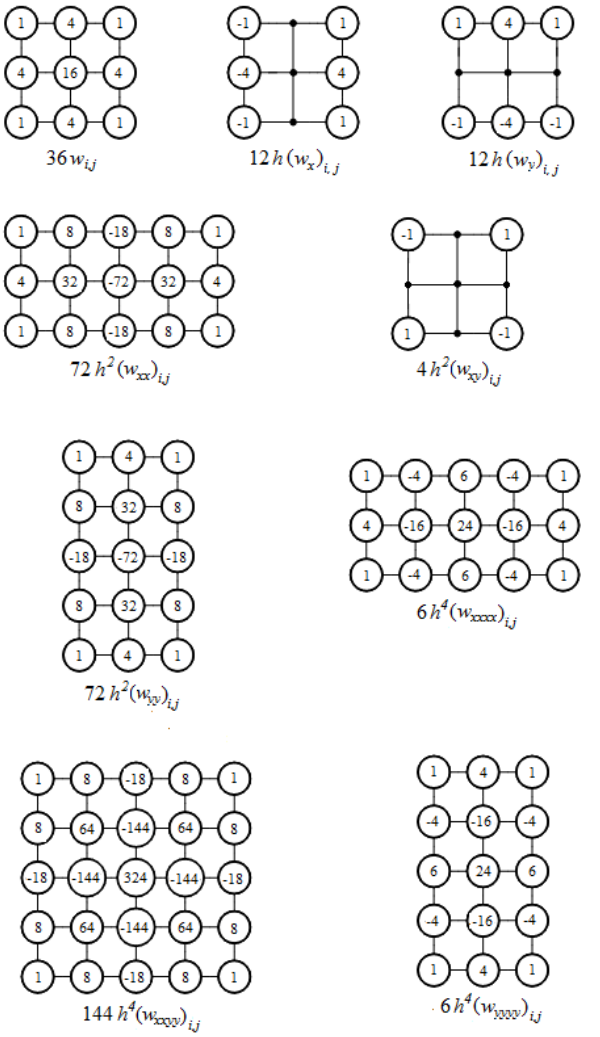

Fig. 5. Schemes for deflection function and its derivatives

Ultimately, coefficients $\tilde{q}_{i,j}$, in each internal node of the mesh (7), can be calculated from algebraic linear system of equations (Kosma 1993, Kosma 2009)

$$\sum_{r=-2}^{2}\sum_{s=-2}^{2} a_{i+r,j+s}\,\tilde{q}_{i+r,j+s} = b_{i,j}\,, \tag{9}$$

for $i=1,2,...,N-1$ and $j=1,2,...,M-1$, where

$$a_{i,j} = 24\alpha_1 + 324\alpha_2 + 24\alpha_3 - 72\alpha_4 - 72\alpha_5\,,$$

$$a_{i-1,j} = a_{i+1,j} = -16\alpha_1 - 144\alpha_2 + 6\alpha_3 + 32\alpha_4 - 18\alpha_5\,,$$

$$a_{i,j-1} = a_{i,j+1} = 6\alpha_1 - 144\alpha_2 - 16\alpha_3 - 18\alpha_4 + 32\alpha_5\,,$$

$$a_{i-1,j-1} = a_{i+1,j+1} = -4\alpha_1 + 64\alpha_2 - 4\alpha_3 + 8\alpha_4 + 8\alpha_5 + \alpha_6\,,$$

$$a_{i+1,j-1} = a_{i-1,j+1} = -4\alpha_1 + 64\alpha_2 - 4\alpha_3 + 8\alpha_4 + 8\alpha_5 - \alpha_6\,,$$

$$a_{i-2,j} = a_{i+2,j} = 4\alpha_1 - 18\alpha_2 + 4\alpha_4\,,$$

$$a_{i,j-2} = a_{i,j+2} = -18\alpha_2 + 4\alpha_3 + 4\alpha_5\,,$$

$$a_{i-2,j-1} = a_{i+2,j-1} = a_{i-2,j+1} = a_{i+2,j+1} = \alpha_1 + 8\alpha_2 + \alpha_4\,,$$

$$a_{i-1,j-2} = a_{i+1,j-2} = a_{i-1,j+2} = a_{i+1,j+2} = 8\alpha_2 + \alpha_3 + \alpha_5\,,$$

$$a_{i-2,j-2} = a_{i+2,j-2} = a_{i-2,j+2} = a_{i+2,j+2} = \alpha_2\,,$$

$$b_{i,j} = \frac{q_{i,j}}{D},$$

$$\alpha_1 = \alpha_3 = \frac{1}{6h^4} \quad , \quad \alpha_2 = \frac{1}{72h^4} \quad ,$$

$$\alpha_4 = -\frac{n_x}{D}\frac{1}{72h^2}, \quad \alpha_5 = -\frac{n_y}{D}\frac{1}{72h^2}, \quad \alpha_6 = -\frac{n_{xy}}{D}\frac{1}{2h^2}.$$

Missing equations in (9) are obtained by the application of boundary conditions. For clamped edges they are in the following form:

$$\tilde{q}_{-1,j} = \tilde{q}_{1,j}\,, \qquad \tilde{q}_{0,j} = -\frac{1}{2}\,\tilde{q}_{1,j}\,.$$

Hence $q_{i,j}$ near the vertices of the plate there are

$$\tilde{q}_{-1,-1} = \tilde{q}_{1,1}\,, \quad \tilde{q}_{-1,0} = \tilde{q}_{0,-1} = -\frac{1}{2}\,\tilde{q}_{1,1}\,, \quad \tilde{q}_{0,0} = \frac{1}{4}\,\tilde{q}_{1,1}\,.$$

Modified coefficients in system of equations (9) in two first inner lines (except for four particular nodes in vertices) e.g. for $i=1$ are

$$\tilde{a}_{-1,j} = \tilde{a}_{0,j} = 0,$$

$$\tilde{a}_{1,j} = 36\,\alpha_1 + 378\,\alpha_2 + 21\,\alpha_3 - 84\,\alpha_4 - 63\,\alpha_5\,,$$

$$\tilde{a}_{1,j+1} = 9\,\alpha_1 - 168\,\alpha_2 - 14\,\alpha_3 - 21\,\alpha_4 + 28\,\alpha_5 + \frac{1}{2}\alpha_6\,,$$

$$\tilde{a}_{1,j-1} = 9\,\alpha_1 - 168\,\alpha_2 - 14\,\alpha_3 - 21\,\alpha_4 + 28\,\alpha_5 - \frac{1}{2}\alpha_6\,,$$

$$\tilde{a}_{1,j-2} = a_{1,j+2} = -21\,\alpha_2 + \frac{7}{2}\alpha_3 + \frac{7}{2}\alpha_5\,.$$

In case of simply supported edges, missing equations in (9) can be obtained analogically from the schemes presented in Fig. 5. while derivatives of accuracy of second rank can be calculated using schemes shown in Fig.6. Hence

$$\tilde{q}_{-1,j} = -\tilde{q}_{1,j}\,, \qquad \tilde{q}_{0,j} = 0;$$

$$\tilde{q}_{-1,-1} = \tilde{q}_{1,1}\,, \qquad \tilde{q}_{-1,0} = \tilde{q}_{0,-1} = \tilde{q}_{0,0} = 0;$$

$$\tilde{a}_{1,j} = 20\,\alpha_1 + 342\,\alpha_2 + 24\,\alpha_3 - 76\,\alpha_4 - 72\,\alpha_5\,,$$

$$\tilde{a}_{1,j+1} = a_{1,j-1} = 5\,\alpha_1 - 152\,\alpha_2 - 16\,\alpha_3 - 19\,\alpha_4 + 32\,\alpha_5\,,$$

$$\tilde{a}_{1,j-2} = a_{1,j+2} = -19\,\alpha_2 + 4\,\alpha_3 + 4\,\alpha_5\,,\ \tilde{a}_{-1,j} = \tilde{a}_{0,j} = 0.$$

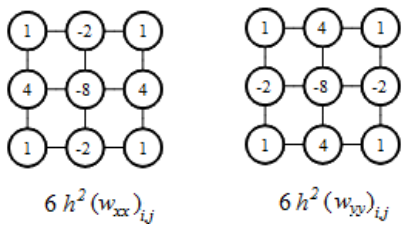

Fig. 6. Scheme for derivatives of accuracy of second rank

System of equations (9), with corresponding missing equations for different edges, is full system that allows to determine function of $w(x,y)$.

3. ALGORITHM VERIFICATION

System of equations (9) with boundary condition equations (5)-(6) are solved with the use of Gauss-Seidel method with subrelaxation parameter equal $\omega = 0.8$ and accuracy $\varepsilon = 1 \cdot 10^{-13}$. Test calculations are obtained for square plate, where $a = b = 1\,m$ and for different values of thicknesses. Mesh in both directions is the same and it is 40×40. Test data are

$$E = 2.06 \cdot 10^{11} \frac{N}{m^2}, \qquad \nu = 0.3,$$
$$q = -1000 \frac{N}{m}, \qquad n_x = n_y = n_{xy} = 0.$$

Convergent solutions are obtained after about 140000 iterations with initial condition $\tilde{q}_{i,j} = q_{i,j}/D$. For all edges clamped results are presented in Table 1 and they are compared to FEM method in Autodesk Simulation v.14 program (mesh with 10000 elements). Sample of results is presented in Fig. 7.

Table 1. Deflection of the plate for all edges clamped

Thickness h[mm]	Deflection z[mm] Proposed Algorithm	Deflection z[mm] Autodesk Simulation v.14
20	– 0.008 379	– 0.008 383
15	– 0.019 861	– 0.019 871
10	– 0.067 031	– 0.067 064
5	– 0.536 253	– 0.536 509

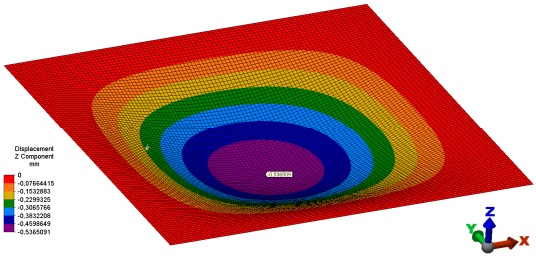

Fig. 7. Sample of results for all edges clamped

Results were also calculated for the plate with all simply supported edges. Convergence was obtained after about 400000 iterations. Deflections with respect to FEM from Autodesk Simulation v.14 are presented in Table 2. Example of deflection is shown in Fig. 8.

Table 2. Deflection of the plate for all simply supported edges

Thickness h[mm]	Deflection z[mm] Proposed Algorithm	Deflection z[mm] Autodesk Simulation v.14
20	– 0.026 839	– 0.026 912
15	– 0.063 623	– 0.063 791
10	– 0.214 724	– 0.215 294
5	– 1.717 773	– 1.722 353

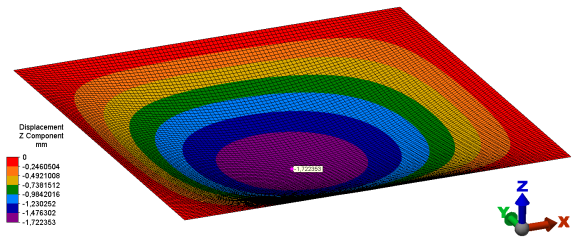

Fig. 8. Sample of results for all edges simply supported

The research revealed that proposed algorithm for calculation of bending of the plate with all clamped or all simply supported edges is efficient.

Additional comparison can be made with approximate analytical solution presented by Timoshenko & Woinowsky-Krieger (1959) for all simply supported edges in the form

$$w_{\max} = 0.0454 \frac{q_0 a^4}{E h^3}.$$

For example for $h = 1\,cm$ we obtain $w_{\max} = -0.221359\ mm$.

However, both methods give only approximate solutions. Therefore, the results obtained with the help of FEM can be treated as a reference solution for *B*-spline approximation method.

4. NUMERICAL EXAMPLE

Above algorithm was used to solve the equation (4) with boundary conditions (6). The plate is build with different number of cells to designate their influence on the deflection (density in cells was higher than in other parts of the plate).

Parameters of the polyethylene plate [Macko 2010]

$$a = b = 0.3m, \quad h = 0.005m,$$
$$E = 1.07 \cdot 10^3 \frac{N}{mm^2}, \quad \nu = 0.41$$

Parameters of the ferrofluid [Stręk 2008]

$$\rho_{PE} = 940 \frac{kg}{m^3}, \quad \rho_f = 1180 \frac{kg}{m^3}, \quad \chi = 0.06 \ ,$$

where ρ_{PE} - density of polyethylene, ρ_f - density of ferrofluid.

Parameters of the magnetic field coils and induced forces. In order to visualize strength in better way, the magnetic field B is in Teslas (and Gausses), not H in amperes per metre.

$$B = 1T = 10000\,Gs,$$
$$B_{x,z} = 0.1 \frac{T}{cm} = 10 \frac{Gs}{cm},$$

$$n_x = 0.03 \frac{N}{m},$$
$$q = \left(-23 - 2.3 \cdot w + q_p\right) \frac{N}{m^2},$$

where q_p is weight of the plate.

Results of some calculation are shown in Table 3 and in Fig. 9.

Table 3. Example of the results

Iter.	Error	Number of cells	w_{max}
630564	9.99986E-14	225 $q_p = -0.441$	– 0.000165
636101	9.99903E-14	900 $q_p = -0.504$	– 0.000180

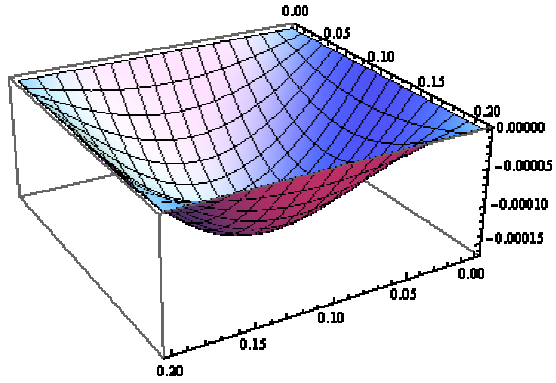

Fig. 9. Bending of the plate under example magnetic field for all edges simply supported

The higher amount of cells with ferrofluid, the bigger fraction of polyethylene in the plate. Hence the load of the plate is smaller and then deflection is smaller as well.

5. CONCLUSIONS

In the paper, model of the plate with cells filled with ferrofluid is presented. The plate is positioned in magnetic field which is generated by system consisting of Helmholtz and Golay coils. Such magnetic field induces forces in the plate in the middle plane and perpendicular to the plate. The solution that takes under consideraton change of magnetic field with deflection of the plate for exemplary plate was presented.

Algorithm using B-spline functions was applied to solve the problem of bending of the plate. This efficiency of proposed method was confirmed by comparison with FEM.

In the paper two numerical methods of different kind are used to solve the eq. (4). Analytical solution is hard to obtain because forces n_x and q depend on coordinates x (in nonlinear way) and z.

ACKNOWLEDGEMENTS

The presented research results, executed under the statutory activities of authors.
Prezentowane wyniki badań, zrealizowane w ramach zadań statutowych autorów

References

1. Ambartsumian S.A., Bagdasarian G.E., Belubekian M.V.: On the magnetoelasticity of thin shells and plates. "Journal of Applied Mathematics and Mechanics" 1973, 37(1), p. 102–118.
2. Czechowski T. et al.: The magnet system for rapid scan electron paramagnetic resonance imaging and spectroscopy. "Concepts in Magnetic Resonance Part B Magnetic Resonance Engineering" 2013, 43B(1).
3. Doyle J.F.: Nonlinear analysis of thin-walled structures: statics, dynamics and stability. New York, Berlin: Springer, 2001.
4. Hasanyan D.J., Harutyunyan S.: Magnetoelastic interactions in a soft ferromagnetic body with a nonlinear law of magnetization: some applications. "International Journal of Solids and Structures" 2009, 46, p 2172–2185.
5. Kaleta J., Materiały magnetyczne Smart: budowa, wytwarzanie, badanie właściwości, zastosowanie. Wrocław: Ofic. Wyd. Pol. Wrocł., 2013.
6. Kędzia P., Magnucki K .:Stateczność płyty prostokątnej pod obciążeniem dynamicznym w polu magnetycznym. „Modelowanie Inżynierskie" 2014, 21(52), s. 107-111.
7. Kosma Z.:Metody i algorytmy numeryczne. Radom: WPR, 2009.
8. Kosma Z.: Rozwiązywanie zagadnień przepływowych metodami funkcji sklejanych. W: Maszyny Przepływowe. T. 13. Wrocław: Ossolineum, 1993.
9. Macko M.: Metoda doboru rozdrabniaczy do materiałów nie-kruchych. "Inż. Ap. Chem." 2010, 49, 5, s. 75-76.
10. Nguyen Q., Tong L.: Voltage and evolutionary piezoelectric actuator design optimization for static shape control of smart plate structures. "Materials & Design" 2007, 28(2), p. 387-39.
11. Rosensweig,R.E.: Ferrohydrodynamics. New York: Cambridge University Press, 1985.

12. Stręk T.: Analiza wymiany ciepła w płynie ferromagnetycznym z wykorzystaniem metody elementów skończonych. Rozprawy. Poznań: Politechnika Poznańska, 2008.
13. Sun D., Tong L.: Design optimization of piezoelectric actuator patterns for static shape control of smart plates. "Smart Material and Structures" 2005, 14(6), p. 1353:1362.
14. Ventsel E., Krauthammer T.: Thin plates and shells: theory, analysis, and applications. New York, Basel: Marcel Dekker, Inc. 2001.
15. Woźniak C. (red.).: Mechanika techniczna. T. 8. Mechanika sprężystych płyt i powłok. Warszawa: Wyd. Nauk. PWN, 2001.
16. You-He Z., Xiaojing Z.: A general expression of magnetic force for soft ferromagnetic plates in complex magnetic fields. "International Journal of Engineering Science" 1997, 35 (15), p. 1405–1417.
17. Timoshenko S., Woinowsky-Krieger S.: Theory of plates and shells. New Yorh: McGraw-Hill Book Company, 1959.